ELSEVIER

Journal of Physics and Chemistry of Solids 63 (2002) 1669–1675

JOURNAL OF
PHYSICS AND CHEMISTRY
OF SOLIDS

www.elsevier.com/locate/jpcs

Heats of solution/substitution of Tl^+, Rb^+, K^+, Br^-, I^- in crystalline CsCl from heats of solid phase transition by differential scanning calorimetry

E.A. Secco[a,*], R.A. Secco[b]

[a]Department of Chemistry, St. Francis Xavier University, P.O. Box 5000, Antigonish, NS, Canada B2G 2W5
[b]Department of Earth Sciences, The University of Western Ontario, London, ON, Canada N6A 5B7

Received 13 August 2001; accepted 5 October 2001

Abstract

Measurements of the change in heat (enthalpy) of transition in crystalline CsCl effected by the presence of guest ions K^+, Rb^+, Tl^+, Br^-, I^- using differential scanning calorimetry are reported. The nature of each mixed-ion solid, 'mixed crystal' or 'crystalline solid solution' is discussed. The limits of solubility of each guest ion are found to be consistent with the subsolidus region described in its respective phase diagram. The quantitative heat of transition values are used to calculate some fundamental solution quantities, viz. slope $\Delta H_t/x$ or $\Delta \bar{H}_{\text{solute}}$, χ, ΔH_S^0, ΔH_L^0—apparent partial molar heat of solution, partial molar heat of solution at infinite dilution, the heat of solution, recovered lattice energy, respectively. © 2002 Elsevier Science Ltd. All rights reserved.

Keywords: D. Phase transitions; C. Differential scanning calorimetry (DSC); C. X-ray diffraction

1. Introduction

The nature of ion–ion interactions in the solid and their effects on the physico-chemical properties of mixed-ion compositions in polymorphic systems involving isostructural compounds is a relatively unexplored area. The existence of a polymorphic substance indicates that the minimum internal energy or cohesive/binding energy of the crystal U_0 does not differ greatly from one structure to another. The enthalpy ΔH_t accompanying the structural transition represents the difference between the cohesive energies of the two structural states, i.e. $U_{0(2)} - U_{0(1)} = \Delta H_t$. The cohesive energy is given by the general expression

$$U_0 = N\left(-\frac{\mathscr{M} Z_i Z_j e^2}{r_0} + \sum_{ij} \lambda_{ij}\, e^{-|r_{ij}|/\rho}\right) \qquad (1)$$

where N is the Avogadro number, $\mathscr{M}$ the Madelung constant for the lattice type, $Z_i Z_j$ the number of charges on given ions i and j, $r_0 = r_i + r_j$, e the electronic charge, r_{ij} the distance separating the ions, λ is the coefficient and ρ a measure of the fall-off of the repulsive potential as a function of the interionic distance. In ionic compounds the dominant interaction is the cation–anion attractive one represented by the first term within the brackets of Eq. (1) while the secondary interactions (cation–cation and anion–anion) are small, of roughly equal importance and are repulsive in nature whose contributions are attributed to the second summation term in Eq. (1). To a first approximation for a M^+X^- type compound hosting a similar guest ion in amounts $0 < x \ll 1.0$ mole fraction Eq. (1) contains the net additional contribution

$$xN\left(-\frac{\mathscr{M} Z_{M^+} Z_{X^-} e^2}{r_{M^+} + r_{X^-}} + \sum_{M^+X^-} \lambda_{M^+X^-}\, e^{-|r_{M^+X^-}|/\rho}\right)$$

in both structures. The presence of a guest in the host would be reflected in the difference in the transition enthalpy between the pure crystal transition and the 'mixed crystal' transition, viz. $\Delta H_{t(\text{pure})} - \Delta H_{t(\text{mixed})} = d(\Delta H_t)$. This latter quantity can lead to the partial molar heat of solution in a crystal at infinite dilution, i.e. χ.

As a continuation of our program on the studies of the

---

* Corresponding author. Tel.: +1-902-8672250; fax: +1-902-8632645.

E-mail address: secco@uwo.ca (E.A. Secco).

PII: S0022-3697(01)00251-7

nature of ion–ion interactions in the solid and their effects on the physico-chemical properties of mixed-ion compositions of polymorphic systems involving isostructural compounds [1–6] we include an investigation on CsCl hosting systems, viz. CsCl–KCl, CsCl–RbCl, CsCl–TlCl, CsCl–CsBr and CsCl–CsI. Two of the relevant factors cited in the solubility/substitution of a guest ion in the host lattice to form a mixed crystal are the similarity in structure of the host and guest compounds, ion property similarity [7] and the effective radius of the guest ion relative to the substituted host ion. All the guest compounds along with CsCl exist only in the cubic structure, space group *Pm*3*m* or *Fm*3*m*. The aim of this study is to measure the relative cohesive energy effect in the CsCl structure by replacing the Cs^+ ion with guest cations of decreasing ionic radius, viz. Rb^+, Tl^+, K^+ where $r_{Cs^+} = 188$ pm, $r_{Rb^+} = r_{Tl^+} = 174$ pm and $r_{K^+} = 165$ pm for C.N. (coordination number) = 8 with a monoatomic Cl^- sublattice relative to that of a polyatomic NO_3^- sublattice where $r_{Cl^-} = r_{NO_3^-} = 171$ pm for C.N. = 8. Also we set out to compare the relative effect on the cohesive energy of the CsCl structure by replacing the Cl^- ion with guest anions of increasing ionic radius, viz. Br^-, I^- where $r_{Br} = 190$ pm and $r_{I^-} = 216$ pm. The differences in the electropositivity and electronegativity of the guest ions may also have an impact on the lattice cohesive energy. The method of analysis of the experimental data from these measurements has already been detailed in earlier reports [4–6].

This report therefore presents the heat of solution/substitution of K^+, Rb^+, Tl^+, Br^-, and I^- in crystalline CsCl along with their recovered lattice energies obtained from heats of transition using differential scanning calorimetry (DSC).

2. Experimental

The compounds used in this study were from the following suppliers with their stated purities: CsCl, Analar (BDH Chemicals), >99.9%; KCl, Alfa Ventron, >99.9%; RbCl, Alfa Ventron, >99.9%; TlCl, Aldrich Chemical, 99%; CsBr, Alfa Ventron, 99%; CsI, Aldrich Chemical, 99.9%. All compositions were prepared by mixing followed by fusing ~50 K above melting in a covered porcelain crucible for ~30 min with slow cooling to room temperature in the furnace over 12 h with power OFF. Each composition of the fused mass was thoroughly ground manually and an aliquot sample was taken for thermal analysis. Random checks after fusion showed no weight loss within limits of weighing error.

Thermal analysis was done with DSC accessory to the DuPont Instrument 9900 Computer/Thermal Analyzer unit for process monitoring, data acquisition and data analysis. The samples encapsulated in copper pans were bathed in flowing N_2 (ultrapure) atmosphere and heated at 10 °C min^{-1}. The melting temperatures and heats of fusion for In and Cd were used as internal references. Repetitive DSC traces of the same pan sample gave ΔH_t values within 0.4% error whereas different pan samples of the same composition gave ΔH_t values within 4% of each other. The transition temperature T_t values of DSC traces agreed within 2 °C for duplicate samples of each composition.

The X-ray diffraction patterns of samples, suspended in methanol using Cu $K_{\alpha 1}$ radiation and dry unsuspended using Co $K_{\alpha 1}$ radiation, obtained at room temperature as described earlier [4,6] gave identical patterns of cubic structure of β-CsCl, *Pm*3*m*. Samples of CsCl–KCl, CsCl–TlCl and CsCl–CsI showed trace peaks of KCl, TlCl and CsI, respectively, along with the dominant pattern characteristic of the room temperature phase β-CsCl. The patterns of CsCl–RbCl and CsCl–CsBr showed only the β-CsCl pattern at room temperature.

3. Results and discussion

The mixed composition diffraction patterns confirm that the host CsCl crystal retains its structure, indicating a straightforward ion substitution on their respective sublattice to form a 'mixed crystal' or 'crystalline solid solution'. In other words, an ideal substitutional solid solution results, permitting the determination of the heat of solution/substitution of the specific guest (solute) ion in the host (solvent) CsCl crystal.

Cesium chloride transforms from the low-temperature *Pm*3*m* structure (β) structure to the high-temperature structure *Fm*3*m* (α) (NaCl structure). There is no observable transition in DSC trace for $Cs_{0.896}K_{0.104}Cl$ up to 520 °C while the transition for $Cs_{0.935}K_{0.065}Cl$ occurs at 365 °C. If there is no transition up to 500 °C as suggested for $x_{KCl} > 0.10$ then this fact indicates that KCl stabilizes the high-temperature CsCl-*Fm*3*m* structure compatible with *Fm*3*m* for KCl over the entire *T*-range of the experiments. In other words the CsCl-*Fm*3*m* structure is stabilized with no evidence of the *Pm*3*m*–*Fm*3*m* transition. No transition is reported in the 1 atm phase diagram [8] of CsCl between 520 °C and the melting temperature at 645 °C. Therefore the stabilized CsCl-*Fm*3*m* structure is stable up to the fusion temperature consistent with its phase diagram and the Condon–Morse potential energy curve [9]. It is interesting to note that $Cs_{0.896}K_{0.104}Cl$ sample after 12 months storage in an air-filled capped glass bottle gave a broad endotherm peak at 464 °C characteristic of pure CsCl. Electrical conductivity measurements showed a transition at ~460 °C paralleling the conductivity behavior in pure CsCl. These facts suggest that the 'mixed crystal' $Cs_{0.896}K_{0.104}Cl$ freshly prepared as fused mass in this study and as single crystal by Weijma and Arends [10] is in a metastable high energy state where slow kinetics operate to effect unmixing/separation. The kinetics for unmixing can be accelerated by X-radiation which can explain the β-CsCl *Pm*3*m* structure pattern with KCl peaks where only the α-CsCl *Fm*3*m* structure pattern

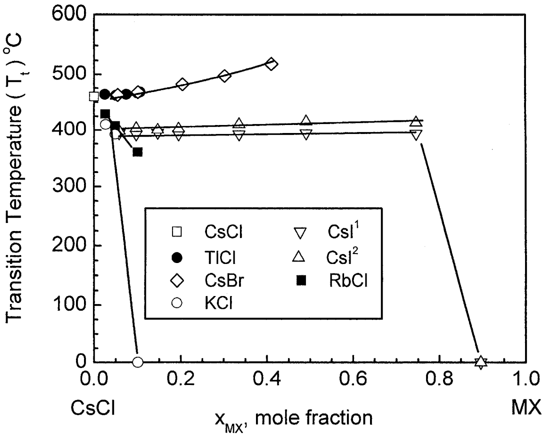

Fig. 1. Plot of transition temperature T_t vs. guest ion mole fraction, x_{MX}, CsCl–MX system; CsI^1 and CsI^2 are described in text.

was expected in the diffraction patterns of $Cs_{0.896}K_{0.104}Cl$. Similarly, the existence of the metastable state and the accelerated effect of X-radiation on the kinetics of unmixing in CsCl–TlCl and CsCl–CsI mixed crystals can account for the trace TlCl and CsI peaks in their diffraction patterns.

3.1. Transition temperature T_t dependence on composition of guest (solute) ion

The transition temperature T_t values cited in the literature range from 445 °C [11,12] to 470–480 °C [12–14] and the transition enthalpy ΔH_t values spread is between $2.43 \pm 0.10\ \text{kJ mol}^{-1}$ and $3.8\ \text{kJ mol}^{-1}$ [10,11,12–18]. Our measured values of T_t and ΔH_t for pure CsCl are 460 ± 2 °C and $2.93 \pm 0.08\ \text{kJ mol}^{-1}$, respectively, reproducible on six traces of samples on different pans. Our ΔH_t values are in excellent agreement with those reported by Weijma and Arends [10], Poyhonen and Mansikka [11], Arell et al. [17] and by Clark [18].

Fig. 1 presents the dependence of the transition temperature T_t as a function of the guest ion mole fraction, x_{MX}, in the CsCl–MX system. T_t approaches linear behavior with increasing Tl^+ and Br^- in the host CsCl while maintaining the cubic β-CsCl structure, *Pm*3*m*, undergoing the $\beta \rightarrow \alpha$, *Pm*3*m* → *Fm*3*m*, transformation. This observation is consistent with the earlier reported phase diagrams by independent workers on CsCl–TlCl [19–22] and CsCl–CsBr [23] along with the differential thermal analysis (DTA) by Weijma and Arends [10]. Our subsolidus temperature behavior for composition region $0 < x_{TlCl} < 0.14$ conforms to the diagram of Ref. [21] but is in contrast to Ref. [22]. On the other hand T_t decreases linearly with increasing KCl and RbCl consistent with earlier reports [24,25]. The subsolidus region of CsI–CsCl diagram is unknown to us. It is relevant to note that our T_t values and limits of solution/substitution of K^+, Rb^+ and Br^- compare very well with those observed by Weijma and Arends [10] using single crystals and their phase diagrams [23–25] which are in marked disagreement with the results for K^+ and Rb^+ reported by Rao et al. [14,15]. Furthermore, the latter results are also inconsistent on the extent of solubility in the subsolidus region of their respective phase diagrams, viz. CsCl–KCl [24] and CsCl–RbCl [25].

The T_t behavior of I^- in CsCl transition represents a special case where T_t decreases to a constant value at $x_{CsI} = 0.10$ and remains constant to $x_{CsI} = 0.80$ and the transition disappears at $x_{CsI} = 0.90$. The limits $0.10 < x_{CsI} < 0.80$ are consistent with the reported phase diagram. Fig. 2 gives DSC traces A and B of $CsCl_{1-x}I_x$ at $x = 0.097$ and 0.509, respectively. Fig. 2A shows the effect of heating 30 min after earlier heat–cool cycle representative of behavior for $x < 0.25$ and Fig. 2B shows the appearance of a distinct doublet representative of behavior for $0.33 < x < 0.80$. The constant T_t values at 393 and 415 °C are consistent with the reported limits of conjugate solid solution presence, CsCl-rich S_1 and CsI-rich S_2 in CsCl–CsI phase diagram [26] and labeled CsI^1 and CsI^2 in Fig. 1. We attribute the endotherm at 415 °C to interaction of S_1 and S_2 to form the 1:1 complex S_1S_2 where the maximum ΔH value occurs at $S_1/S_2 \cong 0.5$. with increasing S_2.

3.2. Enthalpy of transition ΔH_t dependence on composition of guest (solute) ion

The dependence of ΔH_t of the CsCl $\beta \leftrightarrow \alpha$ phase transition on mole fraction x of guest ions K^+, Rb^+, Tl^+, Br^- and I^- is plotted in Fig. 3. The slope of each plot represents the dependence of ΔH_t on mole fraction of guest ion in CsCl lattice, that is, the apparent partial molar heat of solution, $\Delta\bar{H}_{\text{solute}}$, i.e. slope $\Delta H_t/x$. From these molar ΔH_t values we calculate the partial molar heat of solution $d(\Delta H_t)/x$, where $d(\Delta H_t) = \Delta H_{t(CsCl)} - \Delta H_{t(CsCl+guest)}$ with plots of $(d\Delta H_t/x)$ vs. x, mole fraction of guests, Rb^+, Tl^+ and Br^-, K^+ and I^- given in Figs. 4–7, respectively. The aberrant datum at $x = 0.1$ in Fig. 4 is disregarded but it is purposely included to illustrate the limit of the mixed crystal composition required for heat of solution determination. The intercepts of these plots yield the values for the partial molar heat of solution at infinite dilution, χ, of the respective guest ion in CsCl as expressed in

$$\left[\frac{\partial(\Delta H)}{\partial x}\right]_{x=0} = \lim_{x\to 0}\frac{\Delta H}{x} \equiv \chi$$

which leads to ΔH_S^0 from $\Delta H_S^0 = \chi - [\Delta H_f^0(\text{CsCl}) - \Delta H_f^0(\text{guest})]$. It is understood that the ΔH_f^0 quantities are heat/enthalpies of formation from the elements in their standard thermodynamic states. The χ value can also be obtained from the x_{guest} value at the intercept $d(\Delta H_t)/x = 0$ divided into ΔH_t of pure host, viz. CsCl. This x_{guest} value represents the theoretical amount of solute/guest to completely stabilize the high-temperature CsCl α-structure thus eliminating its natural $\beta \rightarrow \alpha$ transition. The consistency between the χ values from the two intercepts, i.e.

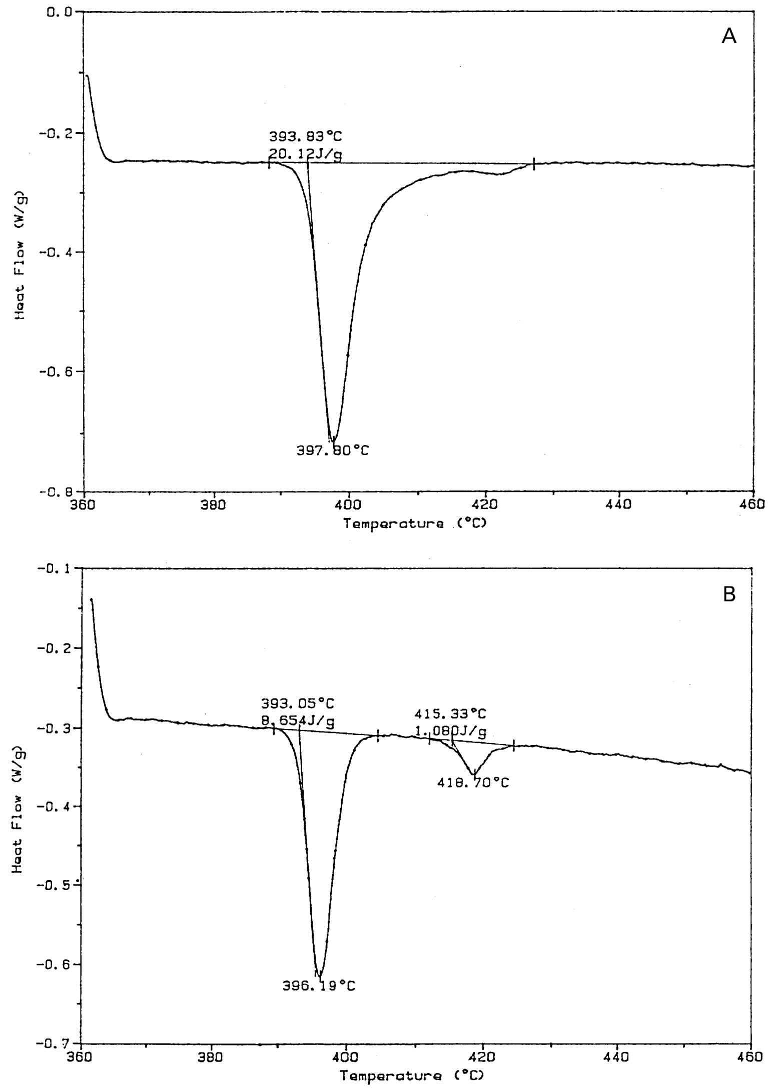

Fig. 2. DSC traces for $CsCl_{0.903}I_{0.097}$, trace A, on second heating and $CsCl_{0.491}I_{0.509}$, trace B, illustrate effect of increasing CsI composition.

$x = 0$ and $d(\Delta H_t)/x = 0$, appears only with Rb^+ in CsCl paralleling earlier consistencies for Rb^+ and Cs^+ in TlI [1,2] and Tl^+ in $RbNO_3$ and Rb^+ in $TlNO_3$ [4,5]. The energetics of Rb^+ solubility in CsCl is in strong contrast with Rb^+ solubility in $CsNO_3$ where $\bar{H}_{Rb^+}$ and χ_{Rb^+} are zero since $\Delta H_{mix} = 0$.

The plots of $d(\Delta H_t)/x$ vs. x for K^+, Tl^+, Br^- and I^- reveal a distinct pattern of solution energetics from Rb^+ in CsCl which is attributed to the specific manner that the CsCl structure responds to accommodating these guest ions. As evident in Fig. 5 the amounts $x_{TlCl} = 0.01$ and $x_{CsBr} = 0.054$ have no impact on ΔH_t of CsCl. This fact is interpreted in terms of ideal solution behavior, i.e. $\Delta H_{mix} = 0$ for these compositions. $\Delta H_{mix} = 0$ for Tl^+ in CsCl parallels the result for Tl^+ in $CsNO_3$ with different composition limits [6]. Passing over the very limited ideal solution regime one can obtain virtual χ values of 6.8 ± 0.3 kJ mol^{-1} for Tl^+ and 0.60 ± 0.05 kJ mol^{-1} for Br^-. The positive slope for Br^- parallels I^-, Fig. 7, indicating an exothermic contribution in the solution process which counters the negative slope observed in all our cation solution/substitution studies [2–6]. The solution of K^+ in CsCl is interpreted as stabilization of the high-temperature α-structure in accordance with its phase diagram [8]. Fig. 6 yields $\chi = 41.5 \pm 3.0$ kJ mol^{-1} and its calculated value from the intercept mole fraction $x_{KCl} = 0.10$ at $d(\Delta H_t)/x = 0$ is 29.3 ± 7.0 kJ mol^{-1}. These values are within the range of $\chi = 32.8$ kJ mol^{-1} calculated from Ref. [10] and shown in Table 1.

The plot of ΔH_t vs. mole fraction CsI, Fig. 3, is consistent with the T_t dependence on x_{CsI}, Fig. 1, and our data extend the region of subsolidus conjugate solutions, S_1 and S_2, in the CsCl–CsI phase diagram [26]. The noteworthy feature is

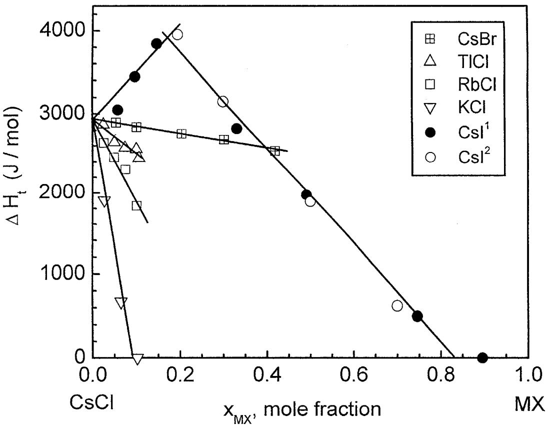

Fig. 3. Plot of transition enthalpy ΔH_t vs. guest ion mole fraction, x_{MX}, in CsCl–MX systems.

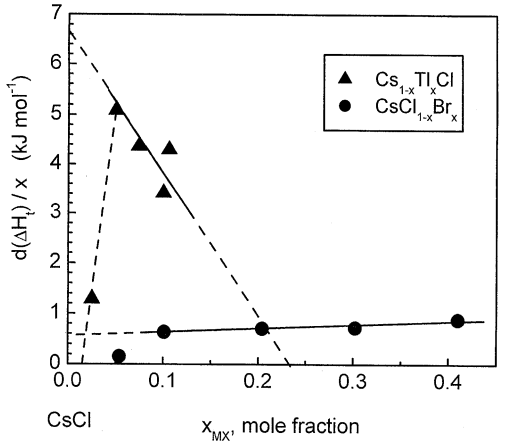

Fig. 5. Plot of partial molar heat of solution $d(\Delta H_t/x)$ vs. mole fraction x of Tl^+ in CsCl and of Br^- in CsCl crystal.

the change of slope from positive, $0 < x_{CsI} < 0.18$, to negative $0.18 < x_{CsI} < 0.80$, for ΔH_t vs. x_{CsI}. The positive slope is for the single phase CsCl-rich whereas the negative slope is for the conjugate solution region, $S_1 + S_2$, attaining $\Delta H_t = 0$ for the single phase CsI-rich. Plotted along with the experimentally measured ΔH_t values in the $S_1 + S_2$ region of Fig. 3 are calculated ΔH_t values for the fraction S_1 phase, open symbols ○ identified by CsI^2, undergoing the $\beta \rightarrow \alpha$ CsCl transformation using the lever principle. The excellent agreement between the measured and calculated ΔH_t is evident and affirms our identification of conjugate solid solutions S_1 and S_2 at $x_{CsI} = 0.18$ and 0.80, respectively.

Values of χ, ΔH_S^0 and recovered lattice energy ΔH_L^0, understood as the destruction of 1 mol of M'X guest lattice and the creation of a new imperfect lattice M'MX, calculated from $\Delta H_L^0 = \chi - [\Delta H_{fL}^0(\text{CsCl}) - \Delta H_{fL}^0(\text{guest})]$ in this study along with some mixed thallium and alkali related compounds for comparison purpose are tabulated in Table 1 where ΔH_{fL}^0 represents heat of formation of the lattice from ions in their standard states, i.e. $U_L = \Delta H_{fL}^0$. Also included in Table 1 are the ΔH_f^0 and ΔH_{fL}^0 values taken from the literature, [12,27–29] except TlCl which was calculated from the Kapustinskii equation, [30] corrected to the transition temperature of the solvent, i.e. 460 °C for CsCl, using the heat capacities of the components [12]. We repeat that only CsCl undergoes a phase transition, viz. CsCl, *Pm*3*m* → *Fm*3*m*, while the remaining compounds maintain their standard state structures to melting temperature.

Attempts to correlate ΔH_S^0 values with ionic radius of the guest ion incorporated in a specific lattice-type have not been successful. It has been suggested that when a larger ion replaces a smaller one the value of ΔH_S^0 is positive [31] as in $Rb^+ \rightarrow K^+$, $Br^- \rightarrow Cl^-$, $Cs^+ \rightarrow Tl^+$ but positive ΔH_S^0 is also observed for smaller ion replacing larger ion, viz.

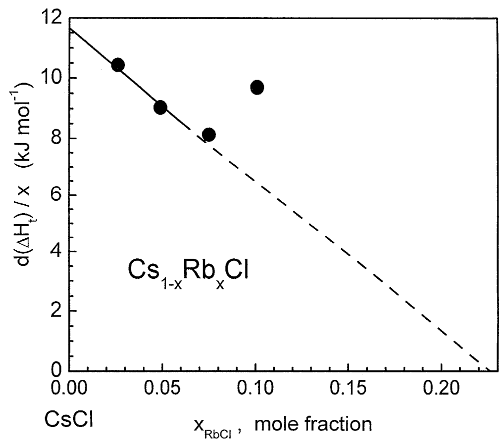

Fig. 4. Plot of partial molar heat of solution $d(\Delta H_t/x)$ vs. mole fraction x of Rb^+ in CsCl crystal.

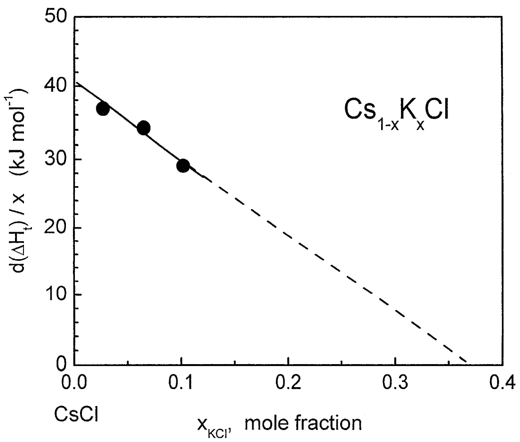

Fig. 6. Plot of partial molar heat of solution $d(\Delta H_t/x)$ vs. mole fraction x of K^+ in CsCl crystal.

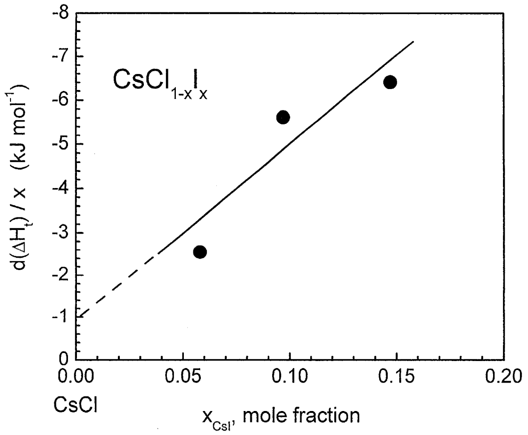

Fig. 7. Plot of partial molar heat of solution $d(\Delta H_t/x)$ vs. mole fraction x of I^- in CsCl crystal.

$K^+ \rightarrow Cs^+$, $Rb^+ \rightarrow Cs^+$, $Tl^+ \rightarrow Cs^+$ as evident in Table 1. A trend between positive ΔH_L^0 values for host ion replacement by a larger guest ion appears in all cases in Table 1. A corollary of this trend is of increasing negative ΔH_L^0 for smaller cations replacing Cs^+ in CsCl from $K^+ \rightarrow Rb^+ \rightarrow Tl^+$. Since $r_{Rb^+} = r_{Tl^+}$ the large difference in ΔH_S^0 cannot be attributed to size factor alone. The values of ΔH_S^0 and ΔH_L^0 and their signs (+ or −) do, however, show their interdependence on the ΔH_f^0 and ΔH_{fL}^0 values, respectively, of the solute and solvent compounds evident in the equation $\Delta H_S^0 = \chi - [\Delta H^0_{f(solvent)} - \Delta H^0_{f(solute)}]$. It would be naive to visualize a simple relationship between relative host–guest ionic size and χ, or H_S^0, or ΔH_L^0 when one considers the interplay of various factors affecting the lattice energy of a given solid composition, viz. dipole–dipole and dipole–quadrapole interactions, attractive and repulsive potentials, relative polarizability, etc. in addition to ionic radius.

In summary, this paper contains additional examples of 'mixed crystal' formation of cations and anions substituted in crystalline CsCl. That is, it provides useful data relevant to ion–ion interaction energies in a common cubic environment to carry out a theoretical analysis of static properties in mixed crystals using the Monte Carlo technique or an approximate quantum approach. The heats of solution terms, viz. $\Delta \bar{H}_{solute}$, χ, ΔH_S^0 and ΔH_L^0 were calculated from quantitative heat of transition measurements using DSC. DSC has been shown once again to be a simple, straightforward and non-destructive solid-state method for reproducible measurements to obtain fundamental enthalpic solution quantities.

Acknowledgements

This study received financial support from Natural Sciences and Engineering Research Council of Canada grants to each author and from the Shell Oil Company of Canada to EAS. EAS is grateful to Prof. M. Steinitz, Physics Department, St. Francis Xavier University for providing laboratory space and facilities in the later stage of this study and to Michael Lewis for technical assistance.

Table 1
Comparison of heats of solution (kJ mol^{-1}) of K^+, Rb^+, Tl^+, Br^-, I^- in CsCl with related metal compounds[a]

Solvent (host)	Solute (guest)	χ (solute)		$\Delta H_S^{0\,a}$	$\Delta H_L^{0\,a}$	$-\Delta H_{fL}^{0\,a}$ (solvent)	Reference
		Intercept at $x = 0$	$d(\Delta H_t/x) = 0 >$				
CsCl	KCl	41.5	29.3	37.5	−8.5	675	This study
CsCl	KCl	32.8	–	–	–	–	[10]
CsCl	RbCl	11.8	12.5	15.0	−21.2	675	This study
CsCl	RbCl	9.5	–	–	–	–	[10]
CsCl	TlCl	0, 6.8[b]	–	257.0	−97.0	675	This study
CsCl	CsBr	0, 0.6[b]	–	38.4	20.8	675	This study
CsCl	CsBr	1.7	–	–	–	–	[10]
CsCl	CsI	−1.0	–	−2.2	49.6	675	This study
$RbNO_3$	$CsNO_3$	6.3	24.2	−10	39.6	759	[5]
$CsNO_3$	$RbNO_3$	0	–	16.3	−33	726	[5]
$TlNO_3$	$CsNO_3$	9.4	19.4	−252	44	759	[5]
$CsNO_3$	$TlNO_3$	0	–	263	−33	726	[5]
$TlNO_3$	$RbNO_3$	11.4	12.7	−258.4	11.4	759	[4]
$RbNO_3$	$TlNO_3$	14.7	16.0	261.7	14.7	759	[4]

[a] All values of ΔH_f and ΔH_{fL} used to calculate ΔH_S^0 and ΔH_L^0 for mixed compositions were corrected to the T_t of the host compound, using their C_p values, i.e. $\int_{298}^{733} \Delta C_p \, dT$.

[b] Virtual values.

References

[1] P.-N. Huang, E.A. Secco, J. Solid State Chem. 103 (1993) 314.

[2] E.A. Secco, A. Sharma, J. Phys. Chem. Solids 56 (1995) 251.

[3] E.A. Secco, J. Phys. Chem. B 101 (1997) 1641.

[4] E.A. Secco, R.A. Secco, Phys. Chem. Chem. Phys. 1 (1999) 5011.

[5] E.A. Secco, R.A. Secco, Phys. Chem. Chem. Phys. 2 (2000) 417.

[6] E.A. Secco, R.A. Secco, J. Phys. Chem. Solids 63 (2002) 433.

[7] C.W. Bunn, Chemical Crystallography, Oxford University Press, London, 1958 p. 59.

[8] L.P. Cook, H.F. McMurdie (Eds.), Phase Diagrams for Ceramists Amer. Ceramic Soc., Inc, Westerville, OH, 1989 No. 7235 and references therein.

[9] J.C. Anderson, K.K. Leaver, R.D. Rawlings, J.M. Alexander, Materials Science, Fourth ed., Chapman and Hall, New York, 1990 p. 132.

[10] H. Weijma, J. Arends, Phys. Status Solidi 35 (1969) 205.

[11] J. Poyhonen, K. Mansikka, Phys. Kondens. Materie 3 (1965) 218.

[12] Selected Values of Chemical Thermodynamic Properties, NBS Circular 500, National Bureau of Standards, Gaithersburg, 1952.

[13] I. Barin, O. Knäcke, O. Kubaschewski, Thermochemical Properties of Inorganic Substances, Springer, Berlin, 1977 p. 250.

[14] M. Natarajan, K.J. Rao, C.N.R. Rao, Trans. Faraday Soc. 66 (1970) 2497.

[15] A.K. Shukla, J.C. Ahluwahlia, C.N.R. Rao, J. Chem. Soc., Faraday Trans. 1 72 (1976) 1288.

[16] C.E. Kaylor, G.E. Walden, D.F. Smith, J. Phys. Chem. 64 (1970) 1960.

[17] A. Arell, M. Roiha, M. Aaltonen, Phys. Kondens. Materie 6 (1967) 140.

[18] S.P. Clark Jr, J. Chem. Phys. 31 (1959) 1526.

[19] C. Sandonnini, Gazz. Chim. Ital. 441 (1914) 323 also in Phase Diagrams for Ceramists, The Amer. Ceramic Soc. No. 1230.

[20] V.A. Isaenko, A.N. Kirgintsev, Zh. Neorg. Khim. 21 (1976) 2493.

[21] V.A. Isaenko, A.N. Kirgintsev, Russ. J. Inorg. Chem. (Engl. Transl.) 21 (1976) 1370 also in Phase Diagrams for Ceramists, The Amer. Ceramic Soc. No 7240.

[22] A. Schiraldi, E. Pezzati, G. Chiodelli, Z. Phys. Chem. (Wiesbaden) 113 (1978) 189 also in Phase Diagrams for Ceramists, The Amer. Ceramic Soc. No. 7241.

[23] J. Sangster, A.D. Pelton, J. Phys. Chem. Ref. Data 16 (3) (1987) 509 also in Phase Diagrams for Ceramists, The Amer. Ceramic Soc. No. 7767(B).

[24] J. Sangster, A.D. Pelton, J. Phys. Chem. Ref. Data 16 (3) (1987) 509 also in Phase Diagrams for Ceramists, The Amer. Ceramic Soc. Nos. 7235 and 7239.

[25] N.B. Chanh, B. DeLuzy de Pelissac, Bull. Soc. Fr. Mineral. Cristallogr. 91 (1968) 13 also in Phase Diagrams for Ceramists, The Amer. Ceramic Soc. Nos. 7238 and 7239.

[26] J.D. Weyand, Diss. Abstr. Int. B 32 (1972) 7014 also in Phase Diagrams for Ceramists, The Amer. Ceramic Soc. No 7801.

[27] J.E. Huheey, Inorganic Chemistry, Third ed., Harper and Row, New York, 1983 p. 67.

[28] D. Cubicciotti, J. Chem. Phys. 31 (1959) 1646.

[29] D. Cubicciotti, J. Chem. Phys. 34 (1961) 2189.

[30] A.F. Kapustinskii, Q. Rev. Chem. Soc. 20 (1956) 203.

[31] D.S. McClure, in: N.B. Hannay (Ed.), Treatise on Solid State Chemistry, 2, Plenum Press, New York, 1975, pp. 5–17.